Chapter 2
On Force-Based Modeling of Pedestrian Dynamics

Mohcine Chraibi, Andreas Schadschneider, and Armin Seyfried

Abstract A brief overview of mathematical modeling of pedestrian dynamics is presented. Hereby, we focus on space-continuous models which include interactions between the pedestrian by forces. Conceptual problems of such models are addressed. Side-effects of spatially continuous force-based models, especially oscillations and overlapping which occur for erroneous choices of the forces, are analyzed in a quantitative manner. As a representative example of force-based models the Generalized Centrifugal Force Model (GCFM) is introduced. Key components of the model are presented and discussed. Finally, simulations with the GCFM in corridors and bottlenecks are shown and compared with experimental data.

2.1 Introduction

The study of pedestrian dynamics has gained special interest due to the increasing number of mass events, where several thousand people gather in restricted areas. In order to understand the laws that govern the dynamics of a crowd several experiments were performed and evaluated. A brief overview can be found in

M. Chraibi (✉)
Jülich Supercomputing Centre, Forschungszentrum Jülich GmbH, 52425 Jülich, Germany
e-mail: m.chraibi@fz-juelich.de

A. Schadschneider
Institute for Theoretical Physics, Universität zu Köln, 50937 Köln, Germany
e-mail: as@thp.uni-koeln.de

A. Seyfried
Jülich Supercomputing Centre, Forschungszentrum Jülich GmbH, 52425 Jülich, Germany

Computer Simulation for Fire Safety and Pedestrian Traffic, Bergische Universität Wuppertal, Pauluskirchstraße 7, 42285 Wuppertal, Germany
e-mail: a.seyfried@fz-juelich.de

S. Ali et al. (eds.), *Modeling, Simulation and Visual Analysis of Crowds*, The International Series in Video Computing 11, DOI 10.1007/978-1-4614-8483-7_2,

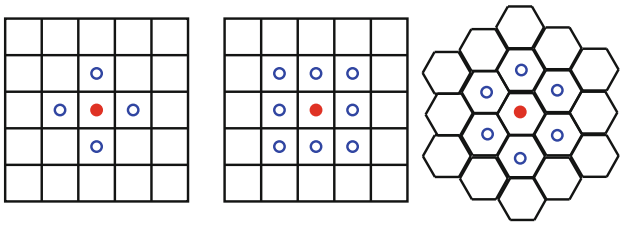

Fig. 2.1 *Left*: Von-Neumann neighborhood. *Middle*: Moore neighborhood. *Right*: Hexagonal neighborhood

[26]. Due to ethical and technical limitations, experimental studies with large numbers of pedestrians are often restricted to controlled labor experiments in specific geometries e.g., bottlenecks [3,10,12,14,15,28,29,35], T-junctions [37] and corridors [1, 5, 31, 38, 39]. Nevertheless, those experiments are beneficial to study quantitative and qualitative properties of pedestrian dynamics. Furthermore, they provide an empirical basis for model development and validation. In fact, validated models can be used to extrapolate the empirical knowledge to cover situations that are difficult to produce with experiments.

Several mathematical models have been developed. Based on their properties, existing models can be categorized into different classes [26]. An increasingly important type of model is based on individual description of pedestrians by means of intrinsic properties and spatial interactions between individuals. Those models state that phenomena which emerge at a macroscopic level arise as a result of interactions at a microscopic level.

Probably, the most investigated microscopic models are the Cellular Automata models (CA), which are "mathematical idealizations of physical systems in which space and time are discrete, and physical quantities take on finite set of discrete values." [34] In the simplest case, CA models decompose space into a rectangular or hexagonal lattice with a cell size of $40 \times 40\,\mathrm{cm}^2$. The state of each cell is described by a discrete variable; "1" for occupied and "0" for empty. It is updated in time according to a set of predefined (stochastic) rules depending on the states of the cells in a certain neighborhood. Depending on the system different neighborhoods can be defined. Figure 2.1 depicts schematically three of the most common neighborhoods used in CA applied to pedestrian dynamics. The full specification of the dynamics of a CA model requires to specify the order in which cells are updated. The most common update strategy is the parallel or synchronous update where all cells are updated at the same time.

CA models describe properties of pedestrian traffic fairly well. However, the discretization of space is not always possible in sensible way. For more details the reader is referred to [27].

Another type of microscopic models which, contrary to CA models, is defined in a continuous space, are force-based models. Force-based models describe the movement of individuals by means of non-linear second-order differential equations. In this chapter, we address properties of force-based models. The question of their realism and ability to describe pedestrian dynamics is discussed in the following.

2.2 Force-Based Models

As early as 1950s, several second-order models has been developed to study traffic dynamics [21–23]. By means of differential equations the *change* of the system with respect to time can be described microscopically by those models. Following Newtonian dynamics, *change* of state results from the existence of exterior forces. As such it can be concluded that the origin of force-based modeling can be traced back to the beginning of the 1950s. An explicit formulation of this forced-based principle in pedestrian dynamics was expressed in [11], who presented a CA-model that "hypothesizes the existence of repulsive forces between pedestrians so that as the subject approaches another pedestrian the 'potential energy' of his position rises and the 'kinetic energy' of his speed drops" [11]. However, the first space-continuous force-based model was introduced by Hirai et al. [8].

Further models for pedestrian dynamics that are based on this force-Ansatz followed [6, 7, 13, 18, 30].

2.2.1 Definition and Issues

Given a pedestrian i with coordinates $\overrightarrow{R_i}$ one defines the set of all pedestrians that influence pedestrian i at a certain moment as $\mathcal{N}_i$ and the set of walls or boundaries that act on i as $\mathcal{W}_i$. In general the forces defining the equation of motion are split into driving and repulsive forces. The repulsive forces model the collision-avoidance performed by pedestrians and should in principle guarantee a certain volume exclusion for each pedestrian. The driving force, on the other hand, models the intention of a pedestrian to move to a certain destination and walk with a desired speed.

Formally the movement of each pedestrian is defined by the equation of motion

$$m_i \frac{d}{dt^2} \overrightarrow{R_i} = \overrightarrow{F_i} = \overrightarrow{F_i}^{\text{drv}} + \sum_{j \in \mathcal{N}_i} \overrightarrow{F_{ij}}^{\text{rep}} + \sum_{w \in \mathcal{W}_i} \overrightarrow{F_{iw}}^{\text{rep}}, \tag{2.1}$$

where $\overrightarrow{F_{ij}}^{\text{rep}}$ denotes the repulsive force from pedestrian j acting on pedestrian i, $\overrightarrow{F_{iw}}^{\text{rep}}$ is the repulsive force emerging from the obstacle w and $\overrightarrow{F_i}^{\text{drv}}$ is a driving force and m_i is the mass of pedestrian i. In [8] the equation of motion (2.1) contains a coefficient of viscosity. However, the influence of this coefficient was not investigated.

For a system of n pedestrians we define the state vector $\overrightarrow{X}(t)$ as

$$\overrightarrow{X}(t) := \begin{pmatrix} \overrightarrow{R_1}(t) \\ \vdots \\ \overrightarrow{R_n}(t) \\ \overrightarrow{v_1}(t) \\ \vdots \\ \overrightarrow{v_n}(t) \end{pmatrix}. \tag{2.2}$$

According to Eq. (2.1) the change of $\overrightarrow{X}(t)$ over time is described by:

$$\frac{d}{dt}\overrightarrow{X}(t) = \begin{pmatrix} \overrightarrow{v}(t) \\ \overrightarrow{F}(t)/m \end{pmatrix}, \tag{2.3}$$

with

$$\overrightarrow{F}(t) = \begin{pmatrix} \overrightarrow{F_1} \\ \vdots \\ \overrightarrow{F_n} \end{pmatrix}, \quad \overrightarrow{v}(t) = \begin{pmatrix} \overrightarrow{v_1} \\ \vdots \\ \overrightarrow{v_n} \end{pmatrix} \quad \text{and} \quad m_i = m \quad \forall i \in [1, n]. \tag{2.4}$$

The state vector at time $t + \Delta t$ is then obtained by integrating (2.3):

$$\overrightarrow{X}(t + \Delta t) = \int_t^{t+\Delta t} \begin{pmatrix} \overrightarrow{v}(\tilde{t}) \\ \overrightarrow{F}(\tilde{t})/m \end{pmatrix} d\tilde{t} + \overrightarrow{X}(t). \tag{2.5}$$

In general the integral in (2.5) may not be expressible in closed form and must be solved numerically.

Force-based models are able to describe qualitatively and quantitatively some aspects of pedestrian dynamics. Nevertheless, they have some conceptual problems. The first problem is Newton's third law. According to this principle two particles interact by forces of equal magnitudes and opposite directions. For pedestrians this law is unrealistic since e.g. normally a pedestrian does not react to pedestrians behind him/her. Even if the angle of vision is taken into account, the forces mutually exerted on each other are not of the same magnitude. In classical mechanics the acceleration of a particle is linear in the force acting on it. Consequently the acceleration resulting from several forces is summed up from accelerations computed from each force. The superposition-principle however, leads to some side-effects when modeling pedestrian dynamics, especially in dense situations where unrealistic backwards movement or high velocities can occur.

Further problems are related to the Newtonian equation of motion describing particles with inertia. This could lead to *overlapping* and *oscillations* of the modeled pedestrians.

On one hand, the particles representing pedestrians can excessively overlap and thus violate the principle of volume exclusion. On the other hand, pedestrians can be pushed backwards by repulsive forces and so perform an oscillating movement towards the exit. This leads to unrealistic behavior especially in evacuation scenarios where a forward movement is dominating. Depending on the strength of the repulsive forces, overlapping and oscillations of pedestrians can be mitigated. However, since both phenomena are related to the repulsive forces this can not be achieved *simultaneously* in a satisfactory way. Reducing the overlapping-issue by increasing the strength of the repulsive forces would lead to an increase of the oscillations in the system. On the other hand, reducing the strength of the repulsive forces may solve the problem of oscillations, but at the same time increase the tendency of overlapping.

In order to solve this overlapping-oscillations duality one can introduce extra rules. One possible solution may be avoiding oscillations by choosing adequate values of the repulsive forces and deal with overlapping among pedestrians with an "overlap-eliminating" algorithm [13]. In [36] a "collision detection technique" was introduced to modify the state variables of the system each time pedestrians overlap with each other. The other possible solution goes in the opposite direction, namely avoiding overlapping by strong repulsive forces and simply eliminate oscillations by setting the velocity to zero [7, 16].

Even if those extra rules may solve the problematic duality, it seems that they are redundant since interactions among pedestrians are no longer expressed only by repulsive forces. This redundancy adds an amount of complexity to the model and is clearly in contradiction to the minimum description length principle [24]. Besides, it is unclear how the modification of the state vector $X(t)$ (2.2) influences the stability of the Eq. (2.5). For those reasons, it is necessary to investigate solutions for the overlapping-oscillations duality without dispensing with the simplicity of the model as originally described with the equation of movement (2.3).

In order to understand the relation between overlapping and oscillations with the repulsive force and hence investigate solutions for the aforementioned problem, we first try to quantify those phenomena and study their behavior with respect to the strength of the repulsive force.

2.2.2 Overlapping

Overlapping is a simulation-specific phenomenon that arises in some models. Unlike CA-models, where volume exclusion is given with the discretization of the space, in poorly calibrated force-based models, unrealistic overlapping between pedestrians are not excluded (Fig. 2.2).

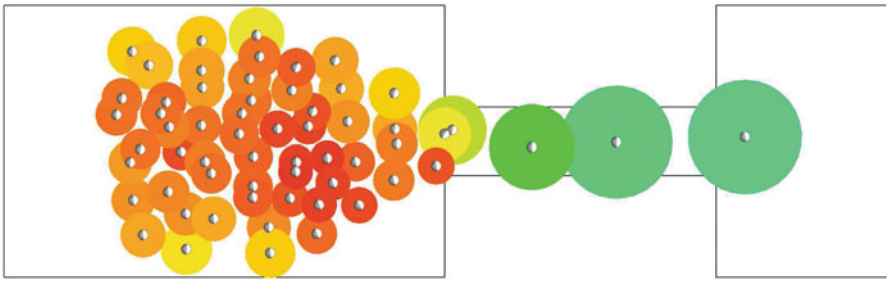

Fig. 2.2 Evacuation through a bottleneck. The simulation screen-shot highlights the problem of excessive overlapping

In order to measure the overlapping that arise during a simulation an "overlapping-proportion" is defined as

$$o^{(v)} = \frac{1}{n_{ov}} \sum_{t=0}^{t_{\text{end}}} \sum_{i=1}^{N} \sum_{j>i}^{N} o_{ij}\,, \tag{2.6}$$

with

$$o_{ij} = \frac{A_{ij}}{\min(A_i, A_j)} \leq 1, \tag{2.7}$$

where N is the number of simulated pedestrians and t_{end} the duration of the simulation. A_{ij} is the overlapping area of the geometrical forms representing i and j with areas A_i and A_j, respectively. n_{ov} is the cardinality of the set

$$\mathscr{O} := \{o_{ij} : o_{ij} \neq 0\}\,. \tag{2.8}$$

For $n_{ov} = 0$, $o^{(v)}$ is set to zero.

2.2.3 Oscillations

Oscillations are backward movements fulfilled by pedestrians when moving under high repulsive forces. Figure 2.3 shows a simulation where pedestrians are force to move in the opposite direction of the exit.

For a pedestrian with velocity $\overrightarrow{v_i}$ and desired velocity $\overrightarrow{v_i^0}$ the "oscillation-proportion" is defined as

$$o^{(s)} = \frac{1}{n_{os}} \sum_{t=0}^{t_{\text{end}}} \sum_{i=1}^{N} S_i\,, \tag{2.9}$$

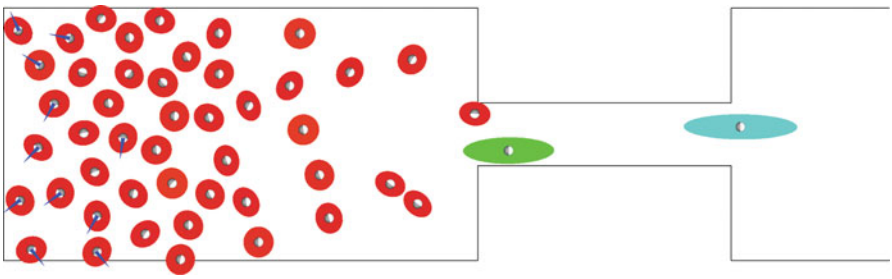

Fig. 2.3 Evacuation through a bottleneck. The simulation screen-shot highlights the problem of oscillations. Note the pedestrians near the walls have the wrong orientation

where S_i quantifies the oscillation-strength of pedestrian i and is defined as follows:

$$S_i = \frac{1}{2}(-s_i + |s_i|)\,, \tag{2.10}$$

with

$$s_i = \frac{\overrightarrow{v_i} \cdot \overrightarrow{v_i}^0}{\| \overrightarrow{v_i^0} \|^2}\,, \tag{2.11}$$

and n_{os} is the cardinality of the set

$$\mathscr{S} := \{s_i : s_i \neq 0\}. \tag{2.12}$$

Here again $o^{(s)}$ is set to zero if $n_{os} = 0$. Note that S_i in Eq. (2.10) is zero if the angle between the velocity and the desired velocity is less that $\pi/2$. This means a realistic deviation of the velocity from the desired direction is not considered as an "oscillation".

The proportions $o^{(v)}$ and $o^{(s)}$ are normalized to 1 and describe the evolution of the overlapping and oscillations during a simulation. The change of $o^{(v)}$ and $o^{(s)}$ is measured with respect to the strength of the repulsive force η. This dependence as well as the overlapping-oscillation duality is showcased in Fig. 2.4.

Increasing the strength of the repulsive force (η) to make pedestrians "impenetrable" leads to a decrease of the overlapping-proportion $o^{(v)}$. Meanwhile, the oscillation-proportion $o^{(s)}$ increases, thus the system tends to become unstable. Large values of the oscillation-proportion $o^{(s)}$ imply less stability. For $s_i = 1$ one has $\overrightarrow{v_i} = -\overrightarrow{v_i}^0$, i.e., a pedestrian moves backwards with desired velocity. Even values of s_i higher than 1 are not excluded and can occur during a simulation.

It should be mentioned that the proportions $o^{(v)}$ and $o^{(s)}$ introduced here are diagnostic tools that help calibrating the strength of the repulsive force in order to minimize overlapping as well as oscillations.

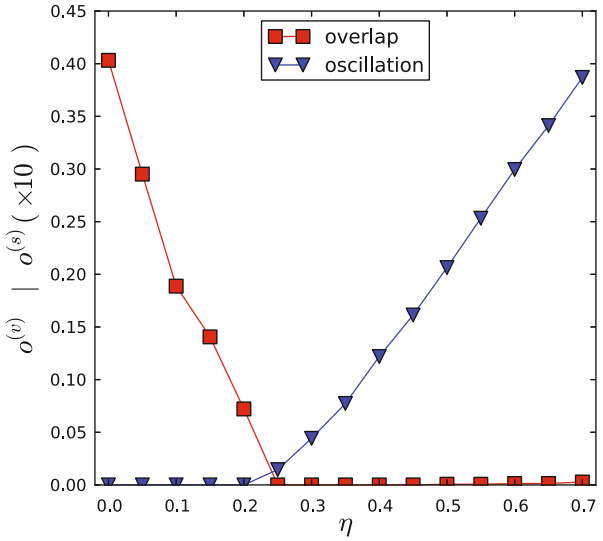

Fig. 2.4 The change of the overlapping-proportion (2.6) and the oscillation-proportion (2.9) in dependence of the repulsive force strength. For each η, 200 simulations were performed

2.3 The Generalized Centrifugal Force Model (GCFM)

The GCFM [2] describes the two-dimensional projection of the human body, by means of ellipses with velocity-dependent semi-axes. It takes into account the distance between the "edges" of the pedestrians as well as their relative velocities. An elliptical volume exclusion has several advantages over a circular one. Because a circle is symmetric with respect to its center, it is inconsistent with the asymmetric space requirement of pedestrians in their direction of motion and transverse to it. One possible remedy would be allowing the center of mass to be different from the geometrical center of the circle. Whether this leads to realistic compliance with the volume exclusion is not clear and should be studied in more detail.

As a force-based model, the GCFM describes the time evolution of pedestrians by a system of superposing short-range forces. Besides the geometrical shape of modeled pedestrians, it emphasizes the relevance of clear model definition without any hidden restrictions on the state variables. Furthermore, quantitative validation, with help of experimental data taken from different scenarios, plays a key role in the development of the model.

2.3.1 Volume Exclusion of Pedestrians

As mentioned earlier, one drawback of circles that impact negatively the dynamics is their rotational symmetry with respect to their centers. Therefore, they occupy

the same amount of space in all directions. In single file movement this is irrelevant since the circles are projected to lines and only the required space in movement direction matters. However, for two-dimensional movement, a rotational symmetry has a negative impact on the dynamics of the system due to unrealistically large lateral space requirements.

In [4] Fruin introduced the "body ellipse" to describe the plane view of the average adult male human body. Pauls [19] presented ideas about an extension of Fruin's ellipse model to better understand and model pedestrian movement as density increases. Templer [32] noticed that the so called "sensory zone", which can be interpreted as a "safety" space between pedestrians and other objects in the environment to avoid physical conflicts and for "psychocultural reasons", varies in size and takes the shape of an ellipse. In fact, ellipses are closer to the projection of required space of the human body on the plane, including the extent of the legs during motion and the lateral swaying of the body. Introducing an elliptical volume exclusion for pedestrians has the advantage over circles (or points) to adjust independently the two semi-axes of the ellipse such that one- and two-dimensional space requirement is described with higher fidelity.

Given a pedestrian i, an ellipse with center (x_i,y_i), major semi-axis a and minor semi-axis b can be defined. a models the space requirement in the direction of movement,

$$a = a_{\min} + \tau_a v_i \tag{2.13}$$

with two parameters $a_{\min}$ and τ_a.

Fruin [4] observed body swaying during both human locomotion and while standing. Pauls [20] remarks that swaying laterally should be considered while determining the required width of exit stairways. In [10], characteristics of lateral swaying are determined experimentally. Observations of experimental trajectories in [10] indicate that the amplitude of lateral swaying varies from a maximum $b_{\max}$ for slow movement and gradually decreases to a minimum $b_{\min}$ for free movement when pedestrians move with their free velocity. Thus with b the lateral swaying of pedestrians is defined as

$$b = b_{\max} - (b_{\max} - b_{\min})\frac{v_i}{v_i^0}. \tag{2.14}$$

Since a and b are velocity-dependent, the inequality

$$b \leq a \tag{2.15}$$

does not always hold for the ellipse i. In the rest of this work we denote the semi-axis in the movement direction by a and its orthogonal semi-axis by b.

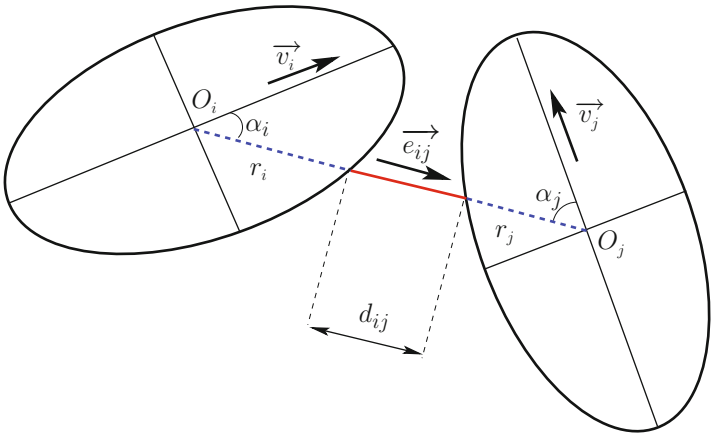

Fig. 2.5 d_{ij} is the distance between the borders of the ellipses i and j along a line connecting their centers

2.3.2 Repulsive Force

Assuming the direction connecting the positions of pedestrians i and j is given by

$$\overrightarrow{R_{ij}} = \overrightarrow{R_j} - \overrightarrow{R_i}, \qquad \overrightarrow{e_{ij}} = \frac{\overrightarrow{R_{ij}}}{\| \overrightarrow{R_{ij}} \|}, \tag{2.16}$$

the repulsive force reads

$$\overrightarrow{F_{ij}}^{\text{rep}} = -m_i k_{ij} \frac{(\eta \| \overrightarrow{v_i^0} \| + v_{ij})^2}{d_{ij}} \overrightarrow{e_{ij}}, \tag{2.17}$$

with the effective distance between pedestrians i and j

$$d_{ij} = \| \overrightarrow{R_{ij}} \| - r_i(v_i) - r_j(v_j). \tag{2.18}$$

r_i is the polar radius of pedestrian i (Fig. 2.5).

This definition of the repulsive force reflects several aspects. First, the force between two pedestrians decreases with increasing distance. In the GCFM it is inversely proportional to their distance (2.18). Furthermore, the repulsive force takes into account the relative velocity v_{ij} between pedestrians i and pedestrian j. The following special definition ensures that for constant d_{ij} slower pedestrians are less affected by the presence of faster pedestrians than by that of slower ones:

$$v_{ij} = \Theta\left((\overrightarrow{v_i} - \overrightarrow{v_j}) \cdot \overrightarrow{e_{ij}}\right) \cdot (\overrightarrow{v_i} - \overrightarrow{v_j}) \cdot \overrightarrow{e_{ij}}, \tag{2.19}$$

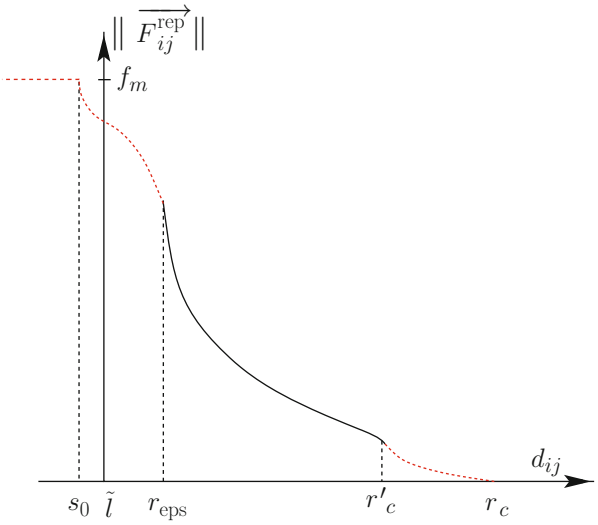

Fig. 2.6 The interpolation of the repulsive force between pedestrians i and j Eq. (2.17) depending on d_{ij} and the distance of closest approach $\tilde{l}$ [40]. As the repulsive force also depends on the relative velocity v_{ij}, this figure depicts the curve of the force for $v_{ij} = \text{const}$. The *right* and *left dashed curves* are defined by a Hermite-interpolation at r_c and r'_{eps}. The wall-pedestrian interaction has an analogous form

with $\Theta()$ is the Heaviside function.

As in general pedestrians react only to obstacles and pedestrians that are within their perception, the reaction field of the repulsive force is reduced to the angle of vision (180°) of each pedestrian, by introducing the coefficient

$$k_{ij} = \Theta(\overrightarrow{v_i} \cdot \overrightarrow{e_{ij}}) \cdot (\overrightarrow{v_i} \cdot \overrightarrow{e_{ij}}) / \parallel \overrightarrow{v_i} \parallel . \tag{2.20}$$

The coefficient k_{ij} is maximal when pedestrian j is in the direction of movement of pedestrian i and minimal when the angle between j and i is bigger than 90°. Thus the strength of the repulsive force depends on the angle.

The interaction of pedestrians with walls is similar to Eq. (2.17). In GCFM walls are treated as three static pedestrians. The number of points is chosen to avoid "going through" walls for pedestrians that are walking almost parallel to walls.

To enhance the numerical behavior of the function (2.17) at small distances a Hermite-interpolation is performed. Furthermore, the force range is reduced to a certain distance r_c. This is especially necessary to avoid summing over distant pedestrians. Figure 2.6 depicts a possible curve of the repulsive force extended by the above mentioned right and left Hermite-interpolation (dashed curves).

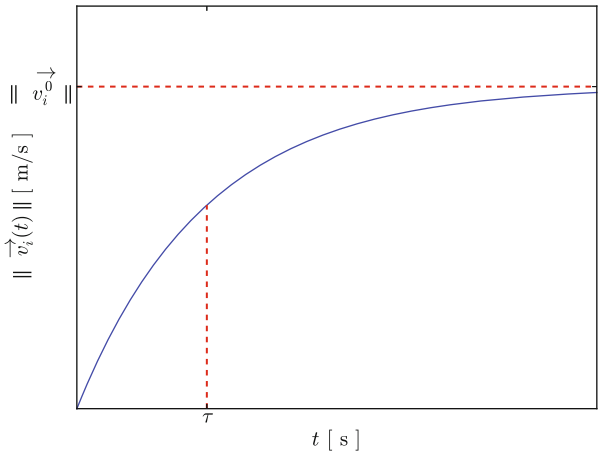

Fig. 2.7 Expected evolution of a pedestrian's velocity with respect to time

2.3.3 Driving Force

From a mathematical standpoint the acceleration of pedestrians may be of different nature e.g., Dirac-like, linear or exponential. According to [21], the later type is more realistic and can take the following expression:

$$\overrightarrow{v_i}(t) = \overrightarrow{v_i^0} \cdot \left(1 - \exp\left(-\frac{t}{\tau}\right)\right), \tag{2.21}$$

with τ a time constant. Figure 2.7 shows the evolution of the velocity in time. See Fig. 2.7.

Differentiation of Eq. (2.21) with respect to t yields

$$\frac{d}{dt}\overrightarrow{v_i}(t) = \frac{1}{\tau} \cdot \overrightarrow{v_i^0} \exp\left(-\frac{t}{\tau}\right). \tag{2.22}$$

From Eq. (2.21) one gets

$$\overrightarrow{v_i^0} \exp\left(-\frac{t}{\tau}\right) = \overrightarrow{v_i^0} - \overrightarrow{v_i}(t). \tag{2.23}$$

Combining (2.22) and (2.23) and considering Newton's second law, the force acting on i with mass m_i is

$$\overrightarrow{F_i}^{\text{drv}} = m_i \frac{\overrightarrow{v_i^0} - \overrightarrow{v_i}}{\tau}. \tag{2.24}$$

This mathematical expression of the driving force, is systematically used in all known force-based models and describes well the free movement of pedestrians. In [33] is has been reported that evaluation of empirical data yields $\tau = 0.61\,\text{s}$. A different value of 0.54 s was reported in [17].

2.4 Steering Mechanisms

In this section the effects of the desired direction on the dynamics by measuring the outflow from a bottleneck with different widths is studied. Two different methods for setting the direction of the desired velocity are discussed.

2.4.1 Directing Towards the Middle of the Exit

This is probably the most obvious mechanism. Herein, the desired direction $\overrightarrow{e_i^0}$ for pedestrian i is permanently directed towards a reference point that exactly lies on the middle of the exit. In some situations it happens that pedestrians can not get to the chosen reference point without colliding with walls. To avoid this and to make sure that all pedestrians can "see" the middle of the exit the reference point e_1 is shifted by half the minimal shoulder length $b_{\min} = 0.2\,\text{m}$ (Fig. 2.8).

Figure 2.9 shows a simulation with 180 pedestrians with this steering mechanism. Even if the entrance of the bottleneck is relatively wide, because of the steering the pedestrians do not make optimal use of the full width and stay oriented towards the middle of the bottleneck.

2.4.2 Mechanism with Directing Lines

In this section we introduce a mechanism that is, unlike the previous one, applicable to all geometries even if the exit point is not visible. Three different lines are

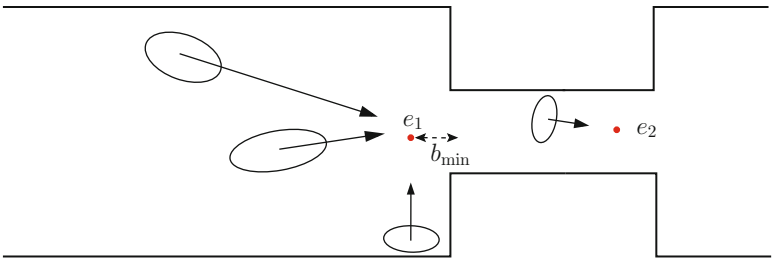

Fig. 2.8 All pedestrians are directed towards the reference points e_1 and e_2

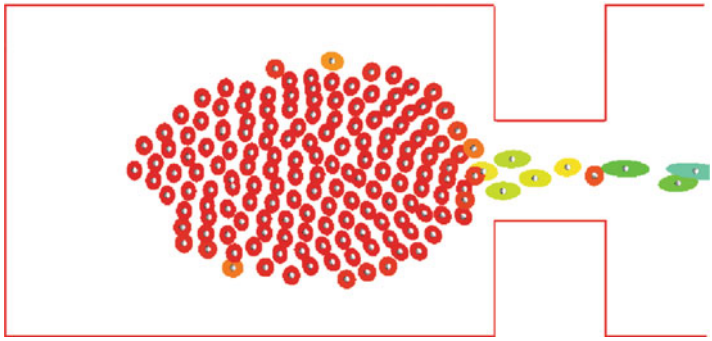

Fig. 2.9 Screen-shot of a simulation. Width of the bottleneck $w = 2.5\,\mathrm{m}$

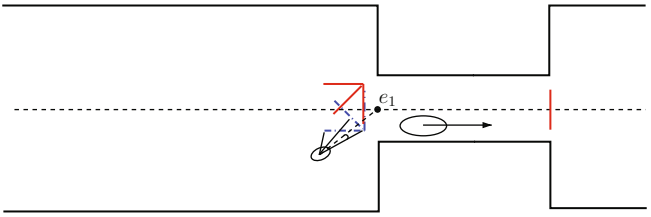

Fig. 2.10 Guiding line segments in front of the generated

defined (Fig. 2.10) which allow to "ease" the movement of pedestrians through the bottleneck. The nearest point from each pedestrian to those lines define its desired direction.

The blue line set (down the dashed line segment) is considered by pedestrians in the lower half and the red line set by pedestrians in the upper half of the bottleneck. For a pedestrian i at position p_i we define the angle

$$\theta_i = \arccos\left(\frac{\overrightarrow{p_i e_1} \cdot \overrightarrow{p_i l_{ij}}}{\| \overrightarrow{p_i e_1} \| \cdot \| \overrightarrow{p_i l_{ij}} \|}\right), \tag{2.25}$$

with l_{ij} the nearest point of the line j to the pedestrian i.

The next direction is then chosen as

$$\overrightarrow{e_i^0} = \frac{\overrightarrow{p_i l_{ij}}}{\| \overrightarrow{p_i l_{ij}} \|} \tag{2.26}$$

with j such that $\theta_j = \min\{\theta_1, \theta_2, \theta_3\}$. The direction lines are shifted in x- and y-direction by $b_{\min}$ to mitigate blocking in the corners.

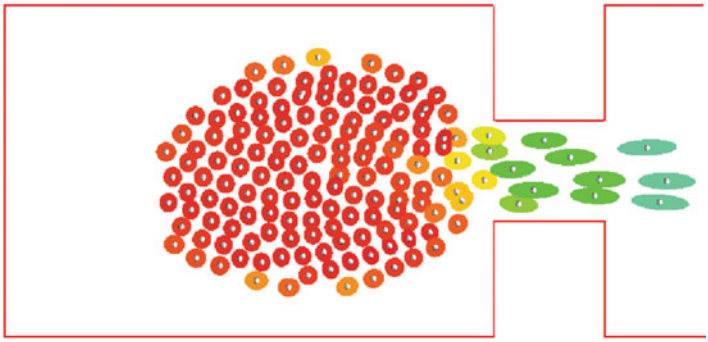

Fig. 2.11 Screenshot of a simulation with directing lines. Width of the bottleneck $w = 2.5\,\mathrm{m}$

Figure 2.11 shows the form of the jam in front of the bottleneck for $w = 2.5\,\mathrm{m}$. In comparison to the first steering mechanism, where pedestrians were direction towards the middle of the bottleneck, here pedestrians make better use of the whole width, which influences the qualitative behavior of pedestrians positively.

2.5 Simulation Results

The free parameters of the model are systematically calibrated by considering single file movement, two dimensional movement in corridors, bottlenecks and corners. In this chapter only simulations results in wide corridors and bottlenecks are presented.

The initial value problem in Eq. (2.1) was solved using an Euler scheme with fixed-step size $\Delta t = 0.01\,\mathrm{s}$. First the state variables of all pedestrians are determined. Then the update to the next step is performed. Thus, the parallelism of the update is ensured.

The desired speeds of pedestrians are Gaussian distributed with mean $\mu = 1.34\,\mathrm{m/s}$ and standard deviation $\sigma = 0.26\,\mathrm{m/s}$. Since there is no uniquely accepted experimental value for the time constant τ in the driving force Eq. (2.24), we set for simplicity $\tau = 0.5\,\mathrm{s}$, i.e. $\tau \gg \Delta t$. The mass m_i is set to unity. In all following simulations the set of parameters is not changed.

To compare the presented steering mechanisms several simulations in a bottleneck are performed. For each mechanisms only the width of the bottleneck is varied from 1 to 2.4 m.

On the basis of a quantitative analysis, the importance of the steering of pedestrians for the observed behavior can be estimated. In the following, for each mechanism the flow through bottlenecks of varying width w is measured. The flow is measured directly at the entrance of the bottleneck according to

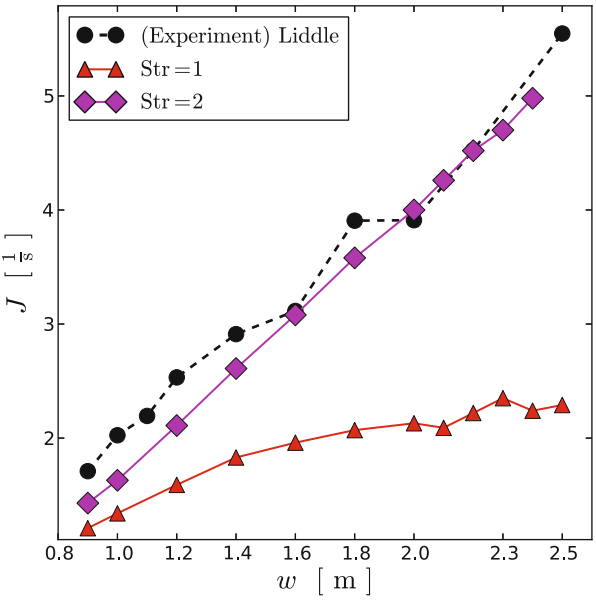

Fig. 2.12 Flow through a bottleneck with different widths

$$J = \frac{N_{\Delta t} - 1}{\Delta t}, \tag{2.27}$$

with $N_{\Delta t} = 180$ pedestrians and Δt the time necessary that all pedestrians pass the measurement line. In Fig. 2.12 the resulting flow in comparison with experimental data is presented.

Keeping the same values of model parameters, the fundamental diagram in a corridor with closed boundary conditions is measured. Here again, for the sake of comparison simulations with circles and ellipses are performed. Results are then validated against experimental data (Figs. 2.13 and 2.14).

2.6 Conclusion and Outlook

In this chapter a brief overview of force-based modeling of pedestrian dynamics is given. Force-based models continuously describe in space the movement of pedestrians by means of differential equations. One can track the origin of this Ansatz back to early 1950s, where first models were developed to describe lane-movement in traffic flow. Since then, force-based models have been successful in describing fairly well the dynamics of pedestrians. Nevertheless, several problems arise from the analogy to Newtonian dynamics. Therefore, principles like superposition, *actio et reactio* should be revised when applied to pedestrian dynamic.

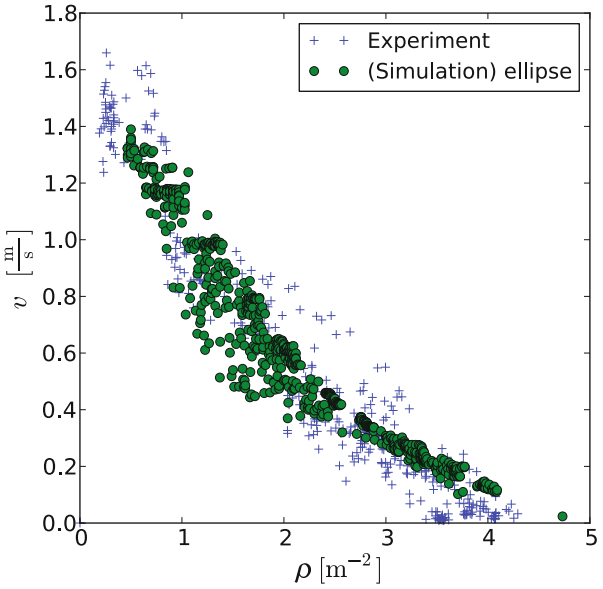

Fig. 2.13 Density-velocity relation with *ellipses* in a corridor of dimensions $25 \times 1\,\mathrm{m}^2$ in comparison with experimental data obtained in the HERMES-project [9, 25]

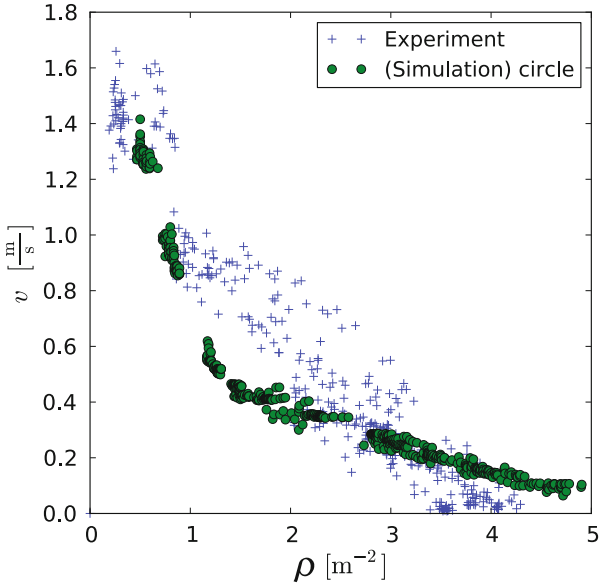

Fig. 2.14 Density-velocity relation with *circles* in a corridor of dimensions $25 \times 1\,\mathrm{m}^2$ in comparison with experimental data obtained in the HERMES-project [9, 25]. In these simulations b is set to be equal to a

By considering the GCFM as an example for force-based models, several important aspects of force-based models were addressed. First, the definition of the repulsive force is presented. By means of a Hermite-interpolation it was possible to overcome the instability of the force at small distances and restrict its range to a maximum distance. Second, several steering mechanism in the driving force are discussed. Finally, simulation results in corridors and bottlenecks are compared to experimental data. It was shown, that it is possible to describe quantitatively pedestrian dynamics in several geometries with *one* set of parameters.

Acknowledgements This work is within the framework of two projects. The authors are grateful to the Deutsche Forschungsgemeinschaft (DFG) for funding the project under Grant-No. SE 1789/1-1 as well as the Federal Ministry of Education and Research (BMBF) for funding the project under Grant-No. 13N9952 and 13N9960.

References

1. Chattaraj, U., Chakroborty, P., Seyfried, A.: Empirical studies on pedestrian motion through corridors of different geometries. In: Proceedings of Transportation Research Board 89th Annual Meeting, CD Rom, Washington, D.C (2010)
2. Chraibi, M., Seyfried, A., Schadschneider, A.: The generalized centrifugal force model for pedestrian dynamics. Phys. Rev. E **82**, 046111 (2010)
3. Daamen, W., Hoogendoorn, S.: Capacity of doors during evacuation conditions. Procedia Eng. **3**, 53–66 (2010)
4. Fruin, J.J.: Pedestrian Planning and Design. Elevator World, New York (1971)
5. Hankin, B.D., Wright, R.A.: Passenger flow in subways. Oper. Res. Soc. **9**(2), 81–88 (1958)
6. Helbing, D.: Collective phenomena and states in traffic and self-driven many-particle systems. Comput. Mater. Sci. **30**, 180–187 (2004)
7. Helbing, D., Molnár, P.: Social force model for pedestrian dynamics. Phys. Rev. E **51**, 4282–4286 (1995)
8. Hirai, K., Tirui, K.: A simulation of the behavior of a crowd in panic. Syst. Control **21**, 409–411 (1977)
9. Holl, S., Seyfried, A.: Hermes – an evacuation assistant for mass events. inSiDe **7**(1), 60–61 (2009)
10. Hoogendoorn, S., Daamen, W.: Pedestrian behavior at bottlenecks. Transp. Sci. **39**(2), 147–159 (2005)
11. Gipps, P.G., Marksjö, B.: A micro-simulation model for pedestrian flows. Math. Comput. Simul. **27**, 95–105 (1985)
12. Kretz, T., Grünebohm, A., Schreckenberg, M.: Experimental study of pedestrian flow through a bottleneck. J. Stat. Mech. Theory Exp. **2006**(10), P10014 (2006)
13. Lakoba, T.I., Kaup, D.J., Finkelstein, N.M.: Modifications of the Helbing-Molnár-Farkas-Vicsek social force model for pedestrian evolution. Simulation **81**(5), 339–352 (2005)
14. Liddle, J., Seyfried, A., Klingsch, W., Rupprecht, T., Schadschneider, A., Winkens, A.: An experimental study of pedestrian congestions: influence of bottleneck width and length. ArXiv e-prints (2009)
15. Liddle, J., Seyfried, A., Steffen, B., Klingsch, W., Rupprecht, T., Winkens, A., Boltes, M.: Microscopic insights into pedestrian motion through a bottleneck, resolving spatial and temporal variations. ArXiv e-prints (2011)
16. Löhner, R.: On the modelling of pedestrian motion. Appl. Math. Model. **34**(2), 366–382 (2010)

17. Moussaïd, M., Helbing, D., Garnier, S., Johansson, A., Combe, M., Theraulaz, G.: Experimental study of the behavioural mechanisms underlying self-organization in human crowds. Proc. R. Soc. B **276**(1668), 2755–2762 (2009)
18. Parisi, D.R., Dorso, C.O.: Morphological and dynamical aspects of the room evacuation process. Physica A **385**(1), 343–355 (2007)
19. Pauls J.L.: Suggestions on evacuation models and research questions. In: Shields, T.J. (ed.) Human Behaviour in Fire. Interscience Communications, London (2004)
20. Pauls J.L.: Stairways and Ergonomics. ASSE, Des Plaines (2006)
21. Pipes, L.A.: An operational analysis of traffic dynamics. J. Appl. Phys. **24**(3), 274–281 (1953)
22. Reuschel, A.: Fahrzeugbewegungen in der Kolonne. Z. Öster. Ing. Arch. **4**, 193–214 (1950)
23. Reuschel, A.: Fahrzeugbewegungen in der Kolonne bei gleichförmig beschleunigtem oder verzögertem Leitfahrzeug. Z. Öster. Ing. Arch. **59**, 73–77 (1950)
24. Rissanen, J.: Minimum-description-length principle. In: Encyclopedia of Statistical Sciences. John Wiley & Sons, Inc., Hoboken (2004)
25. Schadschneider, A.: I'm a football fan ⋯ get me out of here. Phys. World **21**, 21–25 (2010)
26. Schadschneider, A., Klingsch, W., Klüpfel, H., Kretz, T., Rogsch, C., Seyfried, A.: Evacuation Dynamics: Empirical Results, Modeling and Applications. In: Encyclopedia of Complexity and System Science, vol. 5, pp. 3142–3176. Springer, Berlin/Heidelberg (2009)
27. Schadschneider, A., Chowdhury, D., Nishinari, K.: Stochastic Transport in Complex Systems. From Molecules to Vehicles. Elsevier, Amsterdam (2010)
28. Seyfried, A., Passon, O., Steffen, B., Boltes, M., Rupprecht, T., Klingsch, W.: New insights into pedestrian flow through bottlenecks. Transp. Sci. **43**(3), 395–406 (2009)
29. Seyfried, A., Schadschneider, A.: Empirical results for pedestrian dynamics at bottlenecks. In: Wyrzykowski, R., Dongarra, J., Karczewski, K., Wasniewski, J. (eds.) Parallel Processing and Applied Mathematics. Volume 6068 of Lecture Notes in Computer Science, pp. 575–584. Springer, Berlin/Heidelberg (2010)
30. Seyfried, A., Steffen, B., Lippert, T.: Basics of modelling the pedestrian flow. Physica A **368**, 232–238 (2006)
31. Suma, Y., Yanagisawa, D., Nishinari, K.: Anticipation effect in pedestrian dynamics: modelling and experiments. Physica A **391**, 248–263 (2012)
32. Templer, J.A.: The Staircase: Studies of Hazards, Falls, and Safer Design. MIT, Cambridge (1992)
33. Werner, T., Helbing, D.: The social force pedestrian model applied to real life scenarios. In: Galea, E.R. (ed.) Pedestrian and Evacuation Dynamics, pp. 17–26. CMS, London (2003)
34. Wolfram, S.: Statistical mechanics of cellular automata. Rev. Mod. Phys. **55**, 601–644 (1983)
35. Yanagisawa, D., Kimura, A., Tomoeda, A., Ryosuke, A., Suma, Y., Ohtsuka, K., Nishinari, K.: Introduction of frictional and turning function for pedestrian outflow with an obstacle. Phys. Rev. E **80**(3), 036110 (2009)
36. Yu, W.J., Chen, L.Y., Dong, R., Dai, S.Q.: Centrifugal force model for pedestrian dynamics. Phys. Rev. E **72**(2), 026112 (2005)
37. Zhang, J., Klingsch, W., Schadschneider, A., Seyfried, A.: Transitions in pedestrian fundamental diagrams of straight corridors and t-junctions. J. Stat. Mech. (2011). doi:10.1088/1742-5468/2011/06/P06004
38. Zhang, J., Klingsch, W., Seyfried, A.: High precision analysis of unidirectional pedestrian flow within the Hermes project. In: The Fifth Performance-based Fire Protection and Fire Protection Engineering Seminars, Guangzhou, China (2010)
39. Zhang, J., Klingsch, W., Schadschneider, A., Seyfried, A.: Ordering in bidirectional pedestrian flows and its influence on the fundamental diagram. J. Stat. Mech. **2**, P02002 (2012)
40. Zheng, X., Palffy-Muhoray, P.: Distance of closest approach of two arbitrary hard ellipses in two dimensions. Phys. Rev. E **75**(6), 061709 (2007)